IEEE Access
Multidisciplinary : Rapid Review : Open Access Journal

Received March 9, 2022, accepted April 6, 2022, date of publication April 13, 2022, date of current version April 20, 2022.

Digital Object Identifier 10.1109/ACCESS.2022.3167162

# Machine Learning Assisted Characteristics Prediction for Wireless Power Transfer Systems

**SHAMSUL AREFEEN AL MAHMUD, PRASAD JAYATHURATHNAGE, (Member, IEEE), AND SERGEI A. TRETYAKOV, (Fellow, IEEE)**

Department of Electronics and Nanoengineering, School of Electrical Engineering, Aalto University, 02150 Espoo, Finland

Corresponding author: Shamsul Arefeen Al Mahmud (shamsul.almahmud@aalto.fi)

This work was supported in part by the Walter Ahlströmin Säätiö under Grant 20220056; and in part by the Academy of Finland Postdoctoral Researcher under Grant 333479; and in part by the Business Finland Research-to-business under Grant 1527/31/2020.

**ABSTRACT** One of the main challenges in wireless power transfer (WPT) devices is performance degradation when the receiver's position and characteristics vary. Therefore, the load resistance and receiver position must be monitored to ensure proper optimization of power transfer. This study proposes a machine learning (ML) assisted method that estimates the power delivered to the receiver by only using measurements at the transmitter side. Based on the delivered power estimation, we also propose a method to identify if the system efficiency is too low, so that the transmitter should be turned off. This activation control method can be useful in multi-transmitter WPT systems. In addition, we propose an ML method to estimate the load resistance and the coupling coefficient. Using the proposed method, the characteristics of an inductor-capacitor-capacitor (LCC)-Series tuned WPT system are successfully predicted only using the measured root-mean-square and the harmonic contents of the input current. The proposed approach is experimentally validated using a laboratory prototype.

**INDEX TERMS** Wireless power transfer, machine learning, coupling strength estimation, load resistance estimation.

## I. INTRODUCTION

Wireless power transfer (WPT) technology is continuously improving and becoming more common in multiple applications due to a widespread need among both consumers and businesses [1], [2]. In particular, the WPT technology has been recently widely used in biomedical implants [3], consumer electronic devices [4], and electric vehicle charging [5], [6] due to its convenience, flexibility, reliability, and safety.

One of the key challenges in these WPT applications is to create WPT devices capable of transmitting power to freely positioned receivers. The estimation of the power delivered to the receiver is crucial, as the performance degrades when receiver's position and characteristics vary. In WPT systems, the coupling strength between the transmitter (Tx) and receiver (Rx) is the determinant of efficiency: stronger coupling strength between Tx-Rx allows higher power transfer efficiency compared to weak coupling. Moreover, the system characteristics (e.g., efficiency and transferred power) also depend on the load impedance, which may vary depending on the working conditions of the WPT system. For example, the equivalent load resistance of a battery charger depends on the state of charge of the battery. Therefore, knowing the coupling coefficient and load resistance is important for proper optimization of the system performance.

Several methods for the estimation of the output power, coupling coefficient, and load resistance have been proposed in the literature, using voltage and current measurements on both Tx and Rx sides [7], [8], and using additional detector coils on both Tx and Rx sides [9]. However, such approaches need additional sensing devices to detect the presence of Rx and a data communication channel to transfer data of the Rx-side measurements to the Tx-side, which increases costs and complexity. Making such estimations without any Rx-side measurements can greatly simplify the circuits, minimize costs, and increase efficiency.

There have been a few proposed approaches to estimate WPT system parameters only from Tx-side measurements [10]–[17], and a brief comparison of these methods

The associate editor coordinating the review of this manuscript and approving it for publication was Luyu Zhao.

is presented in Table 1. These approaches can be broadly classified to analytical methods [10]–[15], hardware-based synchronization approaches [16], [17] and machine learning assisted methods [18], [19].

Typically, in analytical approaches, results of Tx-side measurements are compared with a theoretical model to estimate WPT link characteristics [10]–[14]. For example, the fundamental harmonic components of the input current and voltage are used to estimate the load voltage or output power in [10]–[12]. One of the prerequisites of the method proposed in [10] is to know initial parameter values such as the coil inductance and parasitic resistances. However, such knowledge of the system is not always available or accurate, which can lead to measurement errors. A current decoupling method is proposed in [13] to control a bidirectional WPT system only from the Tx side measurements, where the mutual inductance is first estimated by varying frequency using a perturbation and observation method, and then changes in the load resistance are continuously monitored by using input current phasor measurements. Such approach can be useful in single-Tx stationary WPT systems, however, it is not applicable to dynamic WPT or multi-Tx WPT systems.

An activation method for multi-Tx WPT systems is proposed in [14], which calculates the mutual inductance ratios between Tx-Rx to find the optimal current distribution in the Tx coils. However, the knowledge of the optimal current ratios is not sufficient to calculate the required optimal values of the currents in the coils. To evaluate the power delivered to the Rx load, one should know the load resistance and the values of the coupling coefficients. In [15], a mathematical approach is proposed to estimate the load and mutual inductance based on transmitter-side parameters, e.g., the input voltage and input current. However, this approach requires to know primary-side parameters, such as inductance, coil resistance, and compensation capacitance. Besides, the analytical method [15] needs current/voltage sensors and current/voltage phase sensors to identify the zero phase angle frequency. Additionally, such analytical methods only consider the fundamental harmonic component, therefore, the accuracy of estimation can be greatly affected due to the presence of higher-order harmonics.

A hardware based approach presented in [16] estimates the coupling coefficient by short-circuiting the active rectifier output momentarily. This method introduces additional control in the receiver side. This study also considered only the fundamental harmonic of the input current.

To the best of our knowledge, only recent study [17] considered the effect of the first- and third-order harmonics in the system analysis to find the output power and mutual coupling. The authors used the direct quadrature transformation technique to acquire fundamental and third harmonic components of the input current. However, in that method, one should know the values of several parameters (such as the inductance and resistances of the coils) beforehand to perform direct quadrature transformation and find the output power or mutual inductance. Therefore, the characterization of the WPT system using only Tx-side measurements by considering higher-order harmonics still remains an important but unsolved problem.

Some machine learning techniques have been employed in recent literature [18], [19] to identify WPT characteristics. In [18], the authors proposed to use online and offline estimation of receiver position by using the knowledge of transmitter coils impedance and optimal activation pattern for known receiver position. This approach requires to know the transmitter parameters and some known position of receiver beforehand so that it is possible to calculate the impedance. Additionally, the method proposed in [19] calculates the efficiency of the system and feed it in the ML estimators. To know the efficiency of the system, one should calculate/measure the parasitic losses of the inductor and capacitors which can be inaccurate. Moreover, no ML based methods have not been proposed to estimate the load resistance, and the effect of higher harmonics in the system has been ignored.

We think that emerging technologies based on artificial intelligence can be applied to address these issues. This paper proposes a simple machine learning assisted method to estimate the mutual coupling between Tx and Rx, the load resistance, and the power delivered to the load, using Tx-side measurements for WPT systems with LCC-tuned Tx. The measured root-mean-square (RMS) value of the input current is used to predict the power delivered to the load, and it is used to decide whether the system operates under high-efficiency conditions or not. If the system efficiency is too low (either because of a very low coupling strength or an extremely low power demand by the receiver), the Tx can be deactivated to avoid energy losses. The proposed deactivation method can be useful in multi-Tx WPT systems where the Tx coils located far away from movable receivers (with low coupling strengths) need to be deactivated. Next, a machine learning based method is proposed to estimate the load resistance and coupling coefficient using the amplitudes and phases of higher-order harmonics of the input current. Such parameter estimations can easily be used for controlling of the power flow to the Rx.

This paper is organised as follows. Section II introduces example LCC-S tuned WPT systems that we consider in this paper and provides the necessary analysis of its characteristics. In Section III the proposed machine learning approach is explained and discussed. In Section IV, the estimation of the output power and the transmitter activation and deactivation method are discussed. In Section V, the ML estimation of the load resistance and coupling coefficient is discussed.

## II. ANALYSIS OF LCC-S WPT SYSTEM

### A. EQUIVALENT CIRCUIT ANALYSIS

The proposed machine learning method is designed and tested for an example of an LCC-series compensated WPT system. This section introduces the system topology and presents an analysis of its characteristics, highlighting the

**TABLE 1. Comparison with recent literature on WPT characteristic estimation methods only from Tx-side measurements.**

| Features | Analytical approaches | | | | | | Hardware based methods | | ML methods | | Proposed method |
|---|---|---|---|---|---|---|---|---|---|---|---|
| | [10] | [11] | [12] | [13] | [14] | [15] | [16] | [17] | [18] | [19] | |
| Independent from model based analysis | x | x | x | x | x | x | ✓ | ✓ | ✓ | ✓ | ✓ |
| No handshaking needed | ✓ | ✓ | x | x | ✓ | ✓ | ✓ | ✓ | ✓ | ✓ | ✓ |
| No initial measurements needed | x | ✓ | ✓ | ✓ | ✓ | x | ✓ | x | x | x | ✓ |
| Effects of higher harmonics | x | x | x | x | x | x | x | ✓ | x | x | ✓ |
| Estimation of output power | ✓ | ✓ | x | x | ✓ | x | x | ✓ | x | x | ✓ |
| Estimation of mutual inductance | x | x | x | ✓ | x | ✓ | ✓ | ✓ | ✓ | ✓ | ✓ |
| Estimation of load resistance | x | x | ✓ | x | x | ✓ | x | x | x | x | ✓ |

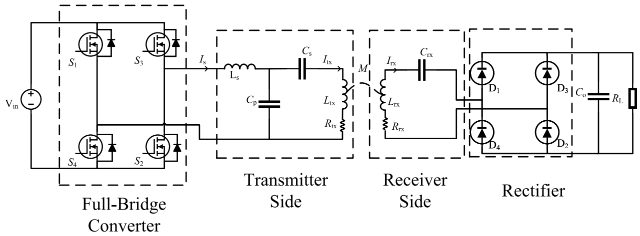


**FIGURE 1. Schematic diagram of an LCC-series tuned WPT system powered by a full-bridge converter.**

effects of higher-order harmonics and parasitic losses in the components. The aim of the analysis is to investigate possibilities of estimating the systems characteristics including 1. power delivered to the load, 2. mutual inductance, and 3. load resistance only from Tx-side measurements.

The LCC-S compensation topology is selected for this study due to its ability to supply load independent constant current [20]. The equivalent circuit of the LCC-S WPT system is illustrated in Fig. 1, where a full-bridge inverter is connected to an LCC-compensated Tx coil, and a series compensated Rx is connected to a load through a full-bridge rectifier. A dc supply ($V_{in}$) is used to drive the inverter.

Typically, the analysis of WPT systems is carried out within the fundamental harmonic approximation and assuming ideal lossless components [21], [22]. Within these assumptions, the input current $I_{\mathrm{s},1}$, the Tx coil current $I_{\mathrm{tx},1}$, and the Rx current $I_{\mathrm{rx},1}$ read [23]

$$I_{\mathrm{s},1} = \frac{M^2 V_\mathrm{s}}{L_\mathrm{s}^2 R_\mathrm{L}}, \quad I_{\mathrm{tx},1} = -j\frac{V_\mathrm{s}}{L_\mathrm{s}\omega_0}, \quad I_{\mathrm{rx},1} = -\frac{M V_\mathrm{s}}{L_\mathrm{s} R_\mathrm{L}} \tag{1}$$

where $V_s$ is the inverter output voltage ($V_a$-$V_b$), $L_\mathrm{s}$ is the Tx-side compensation inductor, $M$ is the mutual inductance between Tx and Rx, $\omega_0$ is the fundamental frequency, and $R_\mathrm{L}$ is the load resistance. The output power delivered to the load resistance can be written as

$$P_\mathrm{out} = I_\mathrm{rx}^2 R_\mathrm{L} \approx \frac{M^2 V_s^2}{L_\mathrm{s}^2 R_\mathrm{L}} \approx I_\mathrm{s} V_s \tag{2}$$

We can see from (2) that the output power is proportional to the input current $I_\mathrm{s}$, assuming the ideal conditions. This property has been used to estimate the power delivered to the load using the input current measurement in paper [14].

However, this idealized system model is not enough accurate for the analysis of the system characteristics in practice. In this work, we will use the currents in different branches at the $n^{th}$ harmonic frequency, which can be derived as

$$\begin{aligned} I_{\mathrm{s},n} &= -\frac{V_{\mathrm{s},n}(R_\mathrm{L} + nR_\mathrm{L}\sigma + \mathrm{j}L\sigma n\omega_0)}{\omega_0(-\mathrm{j}nR_\mathrm{L}\alpha + \sigma(M^2(1+\sigma)^2 + L\alpha)\omega_0)}, \\ I_{\mathrm{tx},n} &= \frac{nV_{\mathrm{s},n}(\mathrm{j}nLR_\mathrm{L}\sigma + M^2 n^4\omega_0 - L^2\sigma^2\omega_0)}{L_\mathrm{s}\omega_0(nR_\mathrm{L}\alpha + \mathrm{j}\sigma(M^2 n^4 + L\alpha)\omega_0)}, \\ I_{\mathrm{rx},n} &= \frac{\mathrm{j}Mn^3 V_{\mathrm{s},n}}{-\mathrm{j}nR_\mathrm{L}\alpha + \sigma(M^2 n^4 + L\alpha)\omega_0} \end{aligned} \tag{3}$$

where $\sigma = n^2 - 1$, $\alpha = L_\mathrm{s} - L\sigma^2$, $L_\mathrm{tx} = L_\mathrm{rx} = L$, and $V_{\mathrm{s},n} = 4V_\mathrm{dc}/n\pi$. $V_{\mathrm{s},n}$ is the $n^{th}$ frequency component of the output voltage of the inverter with the phase shift $\delta = \pi$ between the two legs. These high-order harmonic components of the currents can be substantial under practical working conditions. For example, when the coupling coefficient is very low or the load impedance is very high, the third harmonic component of the input current (i.e., $I_{\mathrm{s},3} \approx -3jV_s/(8L_\mathrm{s}\omega_0)$) can be significant. Therefore, Eq. (1) may not be accurate enough if the coupling coefficient varies. Therefore, it is apparent that the fundamental-harmonic approximation with ideal lossless components is useful only as an initial, very approximate model, and it may not be suitable enough for complete characterization of the power delivered to the load. Furthermore, when the coil losses and multiple harmonics are taken into account, the system model becomes significantly very complex and useless for estimation the system characteristics. Thus, it is necessary to develop alternative methods for parameter estimation, and here we propose a machine-learning approach.

### B. MAKING DECISIONS ON TRANSMITTER ACTIVATION AND DEACTIVATION

When a receiver is far away from the transmitter or the load resistance is very high (low power demand), the power transfer will not be effective, and one should turn off the transmitter. Only when a receiver is enough close to the transmitter coil, Tx should be activated (turned on). This control is particularly important in a multi-Tx scenario to decide which Tx coil is to be activated. In this paper, we train a machine learning model to determine if any given Tx coil

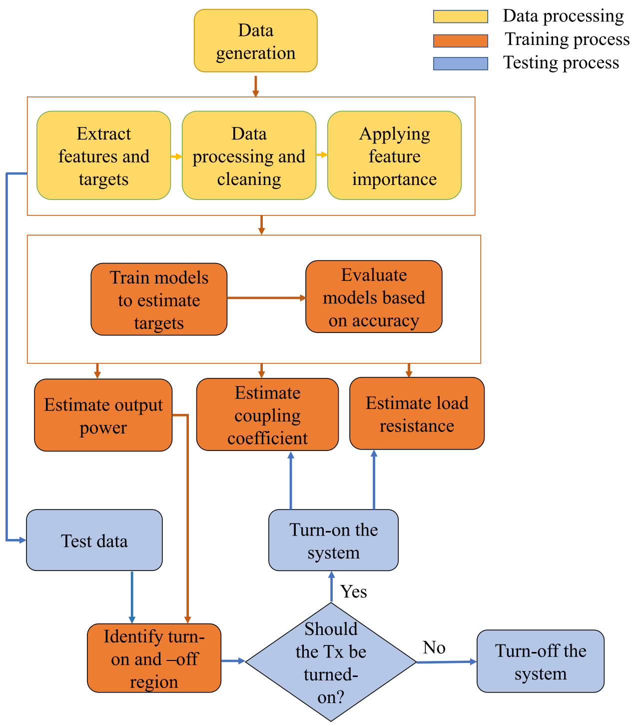


**FIGURE 2. Block diagram of machine learning process.**

needs to be activated or deactivated by analysing the input current of the front-end compensation inductor.

From Equations (1) and (2) it is seen that the output power is proportional to the amplitude of the fundamental harmonic of the input current under ideal conditions. However, it is expected that the relationship may differ in practical situations due to nonlinearities and nonidealities. Moreover, as discussed in Section II-A, higher-order harmonics of the input current can be dominant (e.g., in case of very low coupling strength or very high load resistance). In [24], authors used an equation-based approach to estimate the output power of the system. However, the estimation error becomes significant when the load resistance is high or the coupling strength is low. This problem makes it difficult to estimate the output power using equation-based approaches. In such case, a data-driven approach can offer significant advantages in identification of different characteristics, as it takes into account nonlinearities and nonidealities, as well as higher-order harmonics impact on the system performance. To this end, the proposed machine learning approach is suitable for estimation of the power delivered to the load by analyzing the harmonic content of the input current, allowing making decisions on transmitter activation depending on the power transfer efficiency.

## III. THE MACHINE LEARNING ASSISTED CHARACTERISATION METHOD

### A. THE MACHINE LEARNING APPROACH

The primary purposes of using machine learning in this application are 1. to identify a way to activate and deactivate the transmitter coils depending on the power transfer efficiency; 2. to estimate the power delivered to the load; and 3. to estimate the load resistance and mutual inductance. The proposed machine learning approach is based on measurements of only transmitter-side parameters.

The process of the machine learning approach is illustrated in Fig. 2. The whole process can be divided into three major steps: data processing, training, and testing. At first, training data is generated using LTspice simulation tool and experiments for different combinations of the coupling coefficient $k$ and load resistance $R_L$ values. The data processing stage consists of several steps such as correcting the data format, standardizing the data, removing outliers [25], and extracting features and targets from the raw dataset. Here, *features* mean the parameters that we use to train the model while *targets* refer to the quantities that we want to predict. For instance, we chose the first five harmonic current components and the RMS value of the input current as our features, and the output power $P_{out}$, load resistance $R_L$, and coupling coefficient $k$ as the targets. Once the relevant features and targets are defined, the feature importance analysis is used to identify the best suited features to predict the targets. Feature importance studies are important in predictive modelings, such as machine learning, because they provide insight into the data, information about the model, and the foundation for dimensional reduction and feature selection, which can improve the efficiency and accuracy of predictive models. In this study, nearly 200 data samples from the experiments are used to train ML models. Each sample contains first five harmonic current components and the RMS value of the input current as features, and the output power $P_{out}$, load resistance $R_L$, and coupling coefficient $k$ as targets. Numerous machine learning regression models are considered in this study, for example, random forest, decision tree, support vector machine, adabooster with decision tree [26], and XGboost [27]. The motivation behind using such models is that these models are interpretable while more advanced models like neural network or deep learning models are hardly interpretable [28]. Moreover, the dataset used in this study is quite small which is not a good fit for neural network or deep learning models.

After that, training of the dataset using the best features is done using several machine learning algorithms to find out the most suitable algorithm. 80 % of the data is kept for the training process. The first step of the training phase is to decide if there is a proper receiver in place and if the Tx should be turned on or off, based on the efficiency of the system. If the Tx needs to be turned on, further estimation of the load resistance, and the mutual inductance is carried out.

During the testing phase, a measurement test point is taken and the relevant features are extracted. 20 % of the data is used for testing. Then the features are fed into respective training models to predict the targets. The details of transmitter activation (or deactivation), and estimation of the load resistance and coupling coefficient are further explained in the following section.

**TABLE 2.** Parameters details.

| Description | Design parameters | Experiment parameters |
|---|---|---|
| Tx coil inductance ($L_{tx}$) | 6 $\mu$H | 5.6 $\mu$H |
| Rx coil inductance ($L_{rx}$) | 6 $\mu$H | 5.6 $\mu$H |
| Compensation inductor ($L_s$) | 2.5 $\mu$H | 2.31 $\mu$H |
| Tx coil internal resistance ($R_{tx}$) | 37.7 $m\Omega$ | 34.2 $m\Omega$ |
| Rx coil internal resistance ($R_{rx}$) | 37.7 $m\Omega$ | 35.7 $m\Omega$ |
| Resonant inductor internal resistance ($R_s$) | 15.7 $m\Omega$ | 13.5 $m\Omega$ |
| Input voltage ($V_{in}$) | 10 V | 10 V |
| Switching frequency ($f_s$) | 610 kHz | 605 kHz |
| Resonance frequency ($f_0$) | 600 kHz | 595 kHz |
| Load impedance ($R_L$) | 0.05 $\Omega$ to 200 $\Omega$ | 3 $\Omega$ to 200 $\Omega$ |
| Coupling coefficient ($k$) | 0.02 to 0.5 | 0.05 to 0.5 |

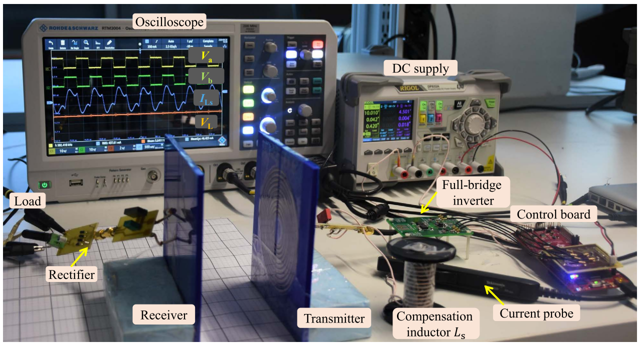


**FIGURE 3.** The experimental setup (Oscilloscope traces show the inverter output voltages $V_a$, $V_b$, the input current $I_s$, and the output voltage $V_L$).

### B. THE EXPERIMENTAL SETUP

The experimental setup shown in Fig. 3 is used for the data generation of the proposed machine learning approach. Two Texas Instrument gallium nitrite (GaN) half bridge FET are used to realize a full bridge inverter. A fixed phase shift angle between the inverter legs at $\pi$ has been selected for this study. However, the same method can be applied for any phase shift angle of the inverter. A current sensor probe (TCP2020) is used to measure the RMS of the input current $I_s$. The parameters of the experimental setup are given in Table 2. During the experiment, the transfer distance and the misalignment distance are varied within the ranges $5-75$ mm and $0-75$ mm, respectively. The diameter of the Tx and Rx coils is 10 cm. The position of the receiver is varied to obtain data for different coupling coefficients ranging approximately from 0.05 to 0.5, and the load resistance $R_L$ is varied from 1 $\Omega$ to 100 $\Omega$. In this study, the RMS of the input current, magnitudes and phases of higher order harmonic contents of the input current, output power, and efficiency data are recorded for different combination of $R_L$ and $k$.

During the experimental study, the magnitudes and phases of the higher harmonics of the input current are extracted using MATLAB by analysing the input current time dependence from oscilloscope. Note that the resonance of the experimental setup is around 595 kHz, which is sightly different from the design frequency of 600 kHz due to experimental disparities in the tuning circuits. This kind of behaviour in practical situations can effectively be handled in machine learning approaches, in contrast to analytical methods.

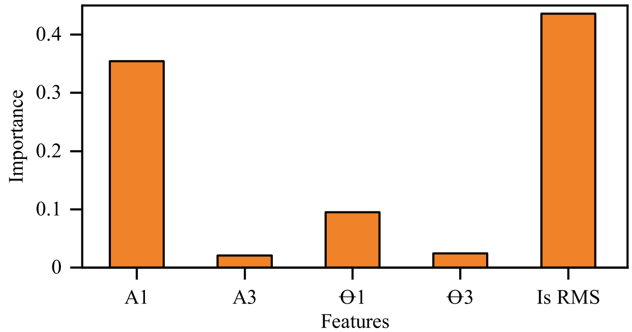


**FIGURE 4.** Features importance for estimating the output power. $A1$ and $A3$ are the magnitudes of the $1^{st}$, and $3^{rd}$ harmonics, $\theta_1$ and $\theta_3$ are the phases of the $1^{st}$ and $3^{rd}$ harmonics, $I_s$RMS is the RMS of the input current $I_s$.

**TABLE 3.** ML models performance for estimating the output power.

| Model Name | Simulation Accuracy (%) | Experimental Accuracy (%) |
|---|---|---|
| Random Forest | 89.31 | 87.5 |
| Decision Tree | 63.15 | 57.07 |
| Support Vector | 71.5 | 67.41 |

## IV. ESTIMATION OF THE OUTPUT POWER AND TRANSMITTER ACTIVATION

This section introduces the proposed method for estimating the power delivered to the load which is needed to make a decision whether to turn the power supplies to the Tx coils on or off.

### A. ESTIMATION OF THE OUTPUT POWER

Here, the goal is to estimate the output power $P_{out}$ using Tx-side measurements. To find a possible approach, a feature importance study is conducted to understand which parameters can be useful to estimate the output power. The results of the study of feature importance are shown in Fig. 4, and it can be seen that RMS of the input current $I_s$ has the highest importance to estimate $P_{out}$.

Figure 5(a) shows the experimentally measured and estimated $P_{out}$ with respect to RMS of $I_s$. For the measurements, the coupling strength $k$ and load resistance $R_L$ are varied within the range given in Table 2. We can clearly see that the predicted output power closely follows the measured one. The estimation accuracies for different regression algorithms are compared in Table 3. The results show that the random forest algorithm gives the highest average accuracy of 88 % for the experimental dataset. Figure 6 shows the individual error for actual vs predict output power. It can be seen that for 90% of the test data the prediction accuracy is above 95%.

The $P_{out}$ vs. $I_s$ profile in Fig. 5(a) clearly shows two distinct regions: the high-power region where $P_{out}$ is linearly increasing with $I_s$, and the low-power region where $P_{out}$ drops sharply with decreasing $I_s$. Interestingly, the efficiency [see $I_s$ profile in Fig. 5(b)] also shows a similar trend: the efficiency is low in the low-power region and it is high in the

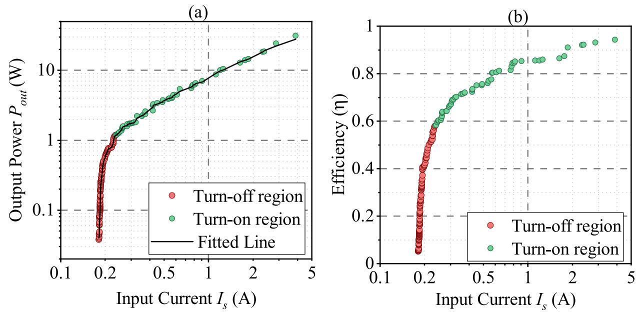


**FIGURE 5. Output power and efficiency variations with respect to the RMS value of $I_S$. (a) Fitted predictive line of the output power; (b) Efficiency against the RMS current. Classification of the "turn-off" (in red color) and "turn-on" regions (in green color) is indicated by different colors.**

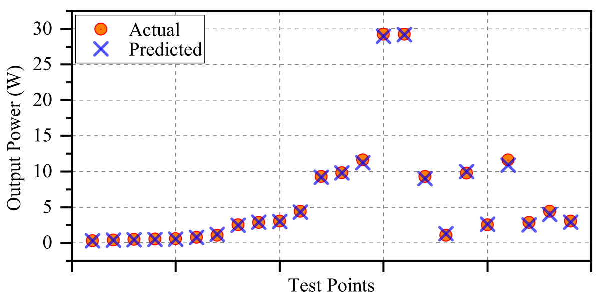


**FIGURE 6. Actual and predicted output power for different test data points.**

high-power region. This low-power region is indeed due to weak coupling or high load resistance (low power demand). It is also observed that the third harmonic component of the input current becomes dominant in the low-power region resulting in this sharp power drop. In fact, understanding all these effects can be encapsulated by using machine learning approach to predict the output power. When the output power drops sharply in the low-power region, the efficiency also drops sharply. This feature is helpful to understand when to turn on or off the transmitter. Low output power or efficiency means that either the receiver is not close to the transmitter or the load power demand is low. Therefore, in this case we should turn off the transmitter. In the following section, transmitter activation (or deactivation) will be discussed.

### *B. TRANSMITTER ACTIVATION*

Next, we need to detect the low-power (and low efficiency) region and make the decision to turn-on or -off the transmitter. It can be seen from Fig. 5 that efficiency is high when the system is operating in the high-power region (marked with green) while the efficiency drops sharply in the low-power region (marked with red). Interestingly, the transition from low power to high power region can corresponds to an elbow point of the $P_{\text{out}}$ vs. $I_{\text{s}}$ curve. The input current at this elbow point of the curve can be used as a threshold to take the decision on activation or deactivation of the Tx.

The random sampling consensus (RANSAC) algorithm is used to identify the high-efficiency region by estimating the linearity of the $P_{\text{out}}$ vs. $I_{\text{s}}$ curve. The RANSAC algorithm is a well-known machine learning method to identify linearity and outliers in the data set [29]. Here, we find the threshold point using the RANSAC algorithm by identifying the elbow point of the $P_{\text{out}}$ vs. $I_{\text{s}}$ curve. The threshold value of the input current identified by the RANSAC algorithm is the determinant for the decision to turn the transmitter on or off. We can see that the turn-on region is characterized by efficiency higher than 60 %, which verifies the efficacy of the proposed method.

In this way, we can estimate the output power and decide whether we should activate or deactivate the Tx coil based only on $I_{\text{s}}$ measurements. This method can also be useful in multi-transmitter WPT systems. In the following section, we will discuss a method of estimating the coupling coefficient and load resistance.

## V. ESTIMATION OF THE COUPLING COEFFICIENT AND LOAD RESISTANCE

Next, the machine learning algorithm is further developed with experimental data for estimation of the coupling coefficient and load resistance. The experimental setup described in Section III-B is used for the data generation and validation of the proposed approach.

### *A. FEATURE STUDY OF THE MACHINE LEARNING METHOD*

It is clear from the discussion in Section II-A that the estimation of the coupling coefficient and load resistance individually is not straightforward using analytical approaches. Therefore, a frequency domain analysis is carried out to understand the effects of different operating frequencies rather than the resonance frequency. For example, Fig. 7 illustrates the frequency response of the input current for a selected set of configurations. At the resonance frequency, the phase angle of the input current is always zero regardless of the load or coupling values. Therefore, if the system is working at the resonance frequency, the phase angle of the input current cannot be used to estimate $k$ or $R_{\text{L}}$. On the other hand, when the operating frequency is slightly lower or higher than the resonance frequency, the phase angle of the input current is different for different $k$ and $R_{\text{L}}$ combinations, which can be used to estimate the load resistance and coupling strength separately. When the system is operating at a slightly higher frequency than the resonance (the inductive region), the switching losses of the inverter become lower [30].

Thus, in this study, we chose to operate the system at a slightly higher frequency than the resonance frequency. The working frequency at 605 kHz is chosen while the resonance frequency is 595 kHz. Once the working regime is different from the system resonance, analytical methods become very complex and not practically useful for the estimations of system parameters. This is yet another reason to introduce a data-driven approach to accurately predict the characteristics

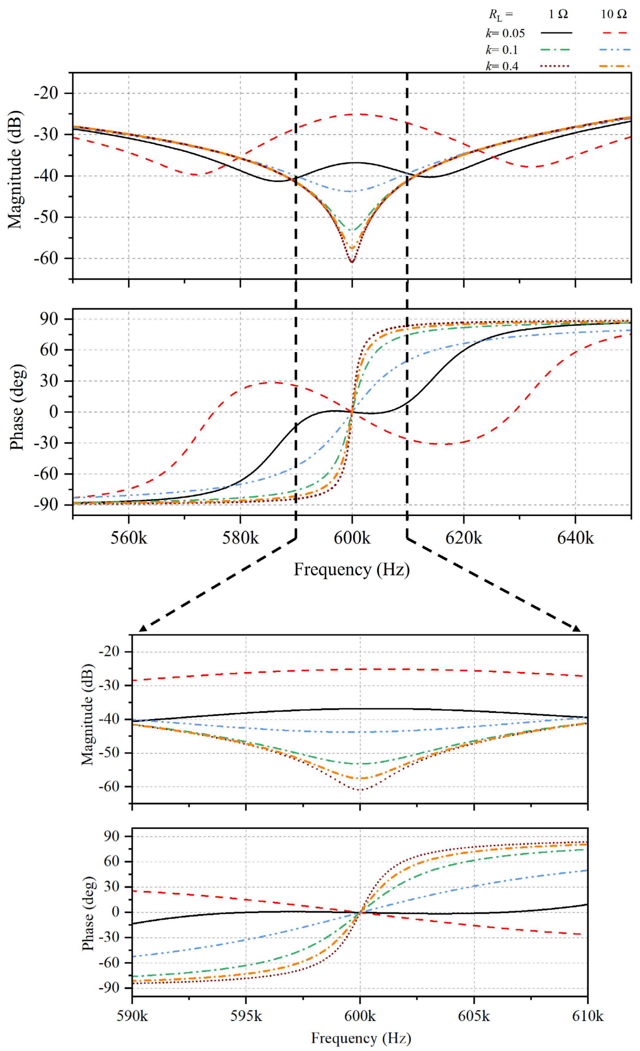


**FIGURE 7.** Frequency-domain analysis of the fundamental harmonic magnitude and phases of the input current $I_s$ for different load resistances and coupling strengths.

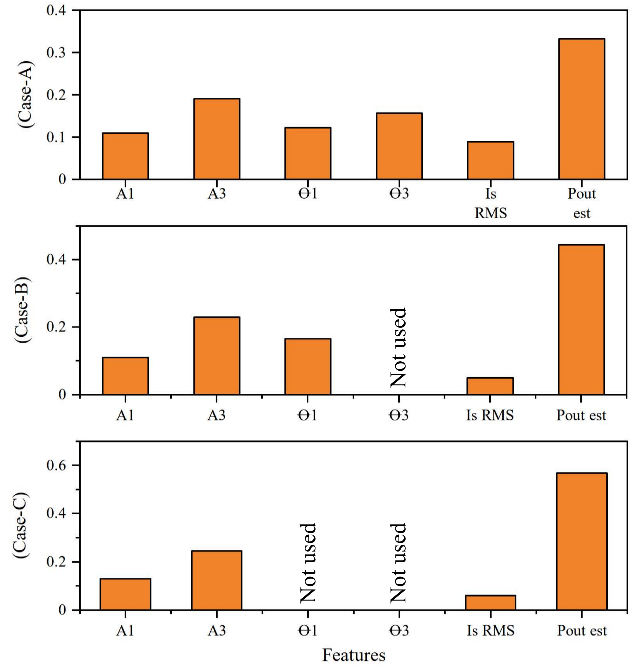


**FIGURE 8.** Features importance on experimental results for estimating the coupling coefficient, where $A1$ and $A3$ are the magnitudes of the $1^{st}$ and $3^{rd}$ harmonics, $\theta_1$ and $\theta_3$ are the phases of the $1^{st}$ and $3^{rd}$ harmonics. The RMS of the input current $I_s$ and the estimated output power $P_{outest}$ from the output power estimation model.

of a WPT system only from the Tx-side measurements, which can effectively account for various nonlinearities and nonidealities.

Next, we chose a set of features related to the input current for estimations of the coupling coefficient and load resistance including amplitudes of first and third harmonic components of the input current ($A1$ and $A3$, respectively), phase of the first and third harmonic components of the input current ($\theta_1$ and $\theta_3$, respectively), the RMS of the input current $I_s$, and the output power estimated from the output power estimation model in previous section $P_{outest}$. Next, a feature importance study is carried out based on well-known sckit-learn random forest regression algorithm to find the appropriate features [31].

Besides, the measurement of the harmonic phases can be experimentally challenging. By considering the measurement complexity, three different cases are considered for the estimation of coupling coefficient and load resistance: *case A* – all the features considered, *case B* – $3^{rd}$ harmonics phase is discarded from the features, and *case C* – both the phases of the $1^{st}$ and $3^{rd}$ harmonics are discarded. The performances of the estimation for different cases and different prediction objectives are discussed in the following sections in detail.

### B. COUPLING COEFFICIENT ESTIMATION

Figure 8 shows a feature importance chart for different case scenarios of coupling coefficient estimations. It can be seen that $P_{outest}$ has the highest importance for all the cases for coupling coefficient estimation. The accuracy of the estimation varies depending on the number of features used in the model.

Several machine learning algorithms including random forest, adabooster with decision tree, and XGboost have been trained to estimate the coupling coefficient using the features shown in Fig. 8. The average accuracy of predictions is shown in Table 4, which will be discussed in detail in Section V-D. Among the used models, adabooster with decision tree shows the best performance with 92% average accuracy for estimating the coupling coefficient. Figure 10(a) shows the actual and predicted coupling coefficient test data points for all the three cases using adabooster with decision tree model. Even in the worst case scenario, the accuracy is higher than 80%. This means that we can accurately predict the coupling coefficient using the proposed machine learning approach.

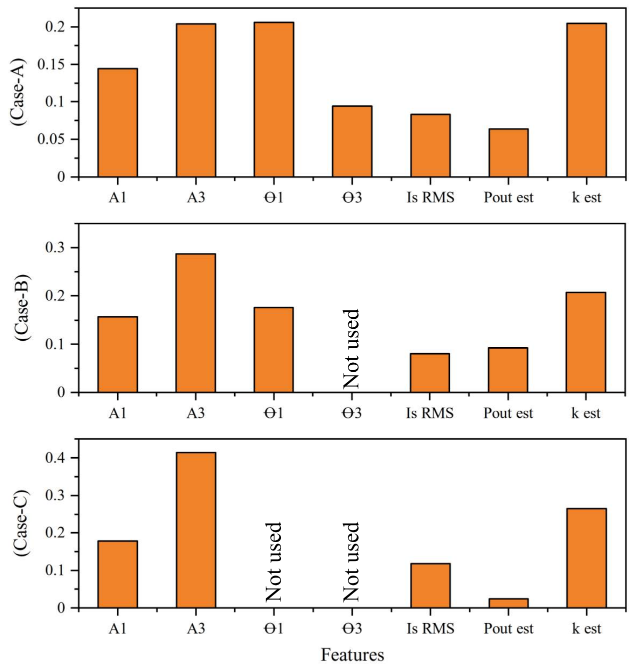


**FIGURE 9.** Features importance of experimental results for estimating the load resistance. $A1$ and $A3$ are the magnitudes of the $1^{st}$ and $3^{rd}$ harmonics, $\theta_1$ and $\theta_3$ are the phases of the $1^{st}$ and $3^{rd}$ harmonics. The RMS of the input current $I_s$, the estimated output power $P_{outest}$ from the output power estimation model and $k_{est}$ from the coupling estimation model.

A detailed discussion on the prediction accuracy and the practicalities is presented in Section V-D.

### C. LOAD RESISTANCE ESTIMATION

The features importance chart to estimate load resistance is shown in Fig. 9 for all three case scenarios. Here, the estimated coupling coefficient $k_{est}$ obtained from the coupling coefficient estimation model described in Section V-B is also used as an additional feature to estimate the load resistance. It can be seen from Fig. 9 that $k_{est}$, $A3$, and $\theta_1$ have the highest importance for load resistance estimations.

Similar to the coupling coefficient estimation, for training to estimations of the load resistance, the features from all three cases are fed into several different algorithms including random forest, adabooster with decision tree, and XGboost. The average accuracy of predictions are shown in Table 4 that will be discussed in details in Section V-D. Among the used methods, adabooster with decision tree shows the best performance with 88% average accuracy for estimating the load resistance. Figure 10(b) shows the actual and predicted load resistance test data points for all the three cases using adabooster with decision tree model. It can be seen that out of 9 test points, 7 have accuracy higher than 80%, while for case C when we omit all the features of phases of the input current, 6 test points out of 9 have accuracy higher than 70%. Thus, the proposed machine learning approach can estimate load resistance of the receiver with a decent accuracy.

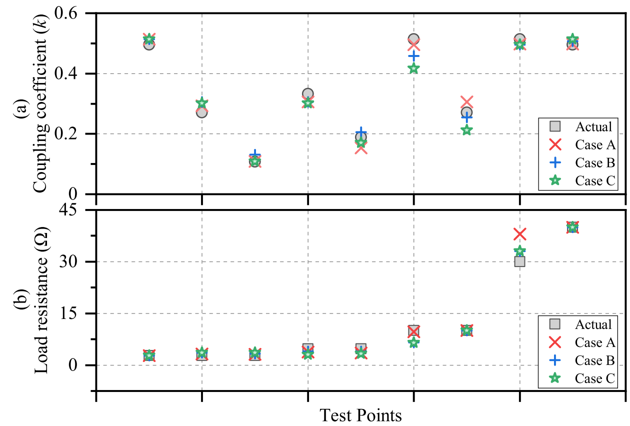


**FIGURE 10.** Actual and predicted (a) coupling coefficient and (b) load resistance for different test points from adabooster with decision tree model.

The prediction accuracy will be discussed in the following section.

### D. DISCUSSION OF RESULTS

It is clear from the above results that different features of the input current can be used to estimate the characteristics of the WPT system. However, measurement complexity of different features can be different. Especially the measurement of the phases of the $1^{st}$ and $3^{rd}$ harmonics could be challenging in applications and may require expensive measurement devices. In this study, three cases are considered to provide options to choose features depending on the application criteria. For example, if the application requires static wireless charging with a highly accurate estimation, then case A would be the wise choice. However, if the application is dynamic charging with moderate prediction accuracy, then case B or C would be the way forward. As we know that in dynamic charging the receiver would move frequently, so the available time to estimate $k$ and $R_L$ would be quite short. In such case, by eliminating measurement of phases can reduce the estimation time, with a slight compromise on the prediction accuracy. For example, the average prediction accuracy of $k$ for the cases A, B, and C are 92%, 91%, and 88%, respectively. Therefore, coupling estimation accuracy is reduced only by 4% in case C. On the other hand, the estimation accuracy of load resistance for the cases A, B, and C are 88%, 85%, and 80%, respectively. Here, case C show 8% reduction of prediction accuracy, however, it is only 3% for case B. The average accuracy of all machine learning models to estimate coupling coefficient and load resistance based on different cases is shown in Table 4.

Therefore, we can conclude that machine learning assisted methods can be used to accurately predict the coupling coefficient and the load resistance without any receiver sensors. By using the proposed estimation method, it is possible to estimate the position of the receiver and, based on this knowledge, the nearby transmitters can be activated and farther away transmitters can be turned off.

**TABLE 4. Average accuracy to estimate coupling coefficient and load resistance with different features.**

| Features | Average accuracy of $k$ | | | Average accuracy of $R_L$ | | |
|---|---|---|---|---|---|---|
| | Case A | Case B | Case C | Case A | Case B | Case C |
| $A_1$ | ✓ | ✓ | ✓ | ✓ | ✓ | ✓ |
| $A_3$ | ✓ | ✓ | ✓ | ✓ | ✓ | ✓ |
| $\theta_1$ | ✓ | ✓ | x | ✓ | ✓ | x |
| $\theta_3$ | ✓ | x | x | ✓ | x | x |
| $I_{sRMS}$ | ✓ | ✓ | ✓ | ✓ | ✓ | ✓ |
| $P_{outest}$ | ✓ | ✓ | ✓ | ✓ | ✓ | ✓ |
| $k_{est}$ | x | x | x | ✓ | ✓ | ✓ |
| Random forest | 83% | 81% | 80% | 81% | 78% | 71% |
| Adabooster DT | 92% | 91% | 88% | 88% | 85% | 80% |
| XGboost | 81% | 79% | 75% | 79% | 80% | 67% |

## VI. CONCLUSION

In this paper, we have proposed a machine learning approach to estimate the power delivered to the load, the coupling coefficient, and the load resistance by using identified transmitter-side parameters. In addition, we introduced a classification allowing transmitter turn-on or -off decisions based on efficiency considerations. The random forest algorithm has been found to offer 90% accuracy of the output power predictions. The RANSAC model has been used to classify the turn-on and turn-off regions for the transmitting coils by identifying the elbow point at the output power-input current curve. Adabooster with decision tree based regression model has the highest accuracy of 88% and 92% in estimations of the load resistance and coupling coefficient, respectively. To enable free positioning of the receiver, knowing the coupling strength is crucial, and the adabooster with decision tree model has the minimum error to estimate that. The outcomes of this work can be used for dynamic tracking of the load status and the coupling of the transmitting coil with the receiving coil in various WPT systems. Importantly, only measurements of transmitter parameters are required, which makes the proposed process simple and straightforward without the need for extra data communication from the receiver side.

## REFERENCES

[1] C. Yang and K. Tsunekawa, "Study of WPT system for charging portable devices on a desk," in *Proc. 10th Int. Symp. Antennas, Propag. EM Theory (ISAPE)*, Oct. 2012, pp. 320–324.

[2] S. Y. R. Hui, W. Zhong, and C. K. Lee, "A critical review of recent progress in mid-range wireless power transfer," *IEEE Trans. Power Electron.*, vol. 29, no. 9, pp. 4500–4511, Sep. 2014.

[3] A. K. R. Rakhyani, S. Mirabbasi, and M. Chiao, "Design and optimization of resonance-based efficient wireless power delivery systems for biomedical implants," *IEEE Trans. Biomed. Circuits Syst.*, vol. 5, no. 1, pp. 48–63, Feb. 2011.

[4] H. Hoang, S. Lee, Y. Kim, Y. Choi, and F. Bien, "An adaptive technique to improve wireless power transfer for consumer electronics," *IEEE Trans. Consum. Electron.*, vol. 58, no. 2, pp. 327–332, May 2012.

[5] C. C. Mi, G. Buja, S. Y. Choi, and C. T. Rim, "Modern advances in wireless power transfer systems for roadway powered electric vehicles," *IEEE Trans. Ind. Electron.*, vol. 63, no. 10, pp. 6533–6545, Oct. 2016.

[6] T. Kan, R. Mai, P. P. Mercier, and C. C. Mi, "Design and analysis of a three-phase wireless charging system for lightweight autonomous underwater vehicles," *IEEE Trans. Power Electron.*, vol. 33, no. 8, pp. 6622–6632, Aug. 2018.

[7] S. Hu, Z. Liang, Y. Wang, J. Zhou, and X. He, "Principle and application of the contactless load detection based on the amplitude decay rate in a transient process," *IEEE Trans. Power Electron.*, vol. 32, no. 11, pp. 8936–8944, Nov. 2017.

[8] D. Kobayashi, T. Imura, and Y. Hori, "Real-time coupling coefficient estimation and maximum efficiency control on dynamic wireless power transfer for electric vehicles," in *Proc. IEEE PELS Workshop Emerg. Technol., Wireless Power*, Daejeon, South Korea, Jun. 2015, pp. 1–6.

[9] A. Azad, A. Echols, V. Kulyukin, R. Zane, and Z. Pantic, "Analysis, optimization, and demonstration of a vehicular detection system intended for dynamic wireless charging applications," *IEEE Trans. Transport. Electrific.*, vol. 5, no. 1, pp. 147–161, Mar. 2019.

[10] X. Meng, D. Qiu, M. Lin, S. C. Tang, and B. Zhang, "Output voltage identification based on transmitting side information for implantable wireless power transfer system," *IEEE Access*, vol. 7, pp. 2938–2946, 2018.

[11] S. Mukherjee, V. P. Galigekere, O. Onar, B. Ozpineci, J. Pries, R. Zeng, and G.-J. Su "Control of output power in primary side LCC and secondary series tuned wireless power transfer system without secondary side sensors," in *Proc. IEEE Energy Convers. Congr. Expo. (ECCE)*, Oct. 2020, pp. 5532–5536.

[12] Z. H. Wang, Y. P. Li, Y. Sun, C. S. Tang, and X. Lv, "Load detection model of voltage-fed inductive power transfer system," *IEEE Trans. Power Electron.*, vol. 28, no. 11, pp. 5233–5243, Nov. 2013.

[13] Y. Liu, U. K. Madawala, R. Mai, and Z. He, "Primary-side parameter estimation method for bidirectional inductive power transfer systems," *IEEE Trans. Power Electron.*, vol. 36, no. 1, pp. 68–72, Jan. 2021.

[14] P. Jayathurathnage and F. Liu, "Optimal excitation of multi-transmitter wireless power transfer system without receiver sensors," in *Proc. IEEE PELS Workshop Emerg. Technol., Wireless Power Transf. (WoW)*, London, U.K., Jun. 2019, pp. 25–28.

[15] Y.-G. Su, L. Chen, X.-Y. Wu, A. P. Hu, C.-S. Tang, and X. Dai, "Load and mutual inductance identification from the primary side of inductive power transfer system with parallel-tuned secondary power pickup," *IEEE Trans. Power Electron.*, vol. 33, no. 11, pp. 9952–9962, Nov. 2018.

[16] Y. Yang, S. C. Tan, and S. Y. R. Hui, "Fast hardware approach to determining mutual coupling of series–series-compensated wireless power transfer systems with active rectifiers," *IEEE Trans. Power Electron.*, vol. 35, no. 10, pp. 11026–11038, Oct. 2020.

[17] J. Liu, G. Wang, G. Xu, J. Peng, and H. Jiang, "A parameter identification approach with primary-side measurement for DC–DC wireless-power-transfer converters with different resonant tank topologies," *IEEE Trans. Transport. Electrific.*, vol. 7, no. 3, pp. 1219–1235, Sep. 2021.

[18] T. Bai, B. Mei, L. Zhao, and X. Wang, "Machine learning-assisted wireless power transfer based on magnetic resonance," *IEEE Access*, vol. 7, pp. 109454–109459, 2019.

[19] H. Shen, P. Tan, B. Song, X. Gao, and B. Zhang, "Receiver position estimation method for multitransmitter WPT system based on machine learning," *IEEE Trans. Ind. Appl.*, vol. 58, no. 1, pp. 1231–1241, Jan. 2022.

[20] Z. Pantic, S. Bai, and S. M. Lukic, "ZCS *LCC*-compensated resonant inverter for inductive-power-transfer application," *IEEE Trans. Ind. Electron.*, vol. 58, no. 5, pp. 3500–3510, Aug. 2011.

[21] C. Xiao, D. Cheng, and K. Wei, "An *LCC-C* compensated wireless charging system for implantable cardiac pacemakers: Theory, experiment, and safety evaluation," *IEEE Trans. Power Electron.*, vol. 33, no. 6, pp. 4894–4905, Jun. 2018.

[22] J. Zhang and F. Wang, "Efficiency analysis of multiple-transmitter wireless power transfer systems," *Int. J. Antennas Propag.*, vol. 2018, pp. 1–11, Jul. 2018.

[23] W. Kim and D. Ahn, "Efficient deactivation of unused LCC inverter for multiple transmitter wireless power transfer," *IET Power Electron.*, vol. 12, no. 1, pp. 72–82, Jan. 2019.

[24] F. Farajizadeh, D. M. Vilathgamuwa, P. Jayathurathnage, and G. Ledwich, "Estimation of the transferred power in LCC compensated wireless power transmitters with the use of PWM-synchronized sampling technique," *IEEE Trans. Transport. Electrific.*, vol. 8, no. 1, pp. 710–722, Mar. 2022.

[25] M. Z. H. Jesmeen, J. Hossen, S. Sayeed, C. K. Ho, K. Tawsif, A. Rahman, and E. Arif, "A survey on cleaning dirty data using machine learning paradigm for big data analytics," *Indonesian J. Elect. Eng. Comput. Sci.*, vol. 10, no. 3, pp. 1234–1243, Jun. 2018.

[26] *1.11. Ensemble methods*. Accessed: Apr. 8, 2022. [Online]. Available: https://scikit-learn/stable/modules/ensemble.html

[27] *Python API Reference—XGBoost 1.5.2 Documentation*. Accessed: Apr. 8, 2022. [Online]. Available: https://xgboost.readthedocs.io/en/stable/python/python_api.html

[28] N. Burkart and M. F. Huber, ''A survey on the explainability of supervised machine learning,'' *J. Artif. Intell. Res.*, vol. 70, pp. 245–317, Jan. 2021. [Online]. Available: https://jair.org/index.php/jair/article/view/12228

[29] S. Debnath, A. Banerjee, and V. Namboodiri, ''Adapting RANSAC SVM to detect outliers for robust classification,'' in *Proc. Brit. Mach. Vis. Conf.*, Swansea, U.K., 2015, pp. 168.1–168.11.

[30] J. A. Sabate, V. Vlatkovic, R. B. Ridley, and F. C. Lee, ''High-voltage, high-power, ZVS, full-bridge PWM converter employing an active snubber,'' in *Proc. 6th Annu. Appl. Power Electron. Conf. Exhib. (APEC)*, Mar. 1991, pp. 158–163.

[31] F. Pedregosa, G. Varoquaux, A. Gramfort, V. Michel, B. Thirion, O. Grisel, M. Blondel, P. Prettenhofer, R. Weiss, V. Dubourg, J. Vanderplas, A. Passos, D. Cournapeau, M. Brucher, M. Perrot, and E. Duchesnay, ''Scikit-learn: Machine learning in Python,'' *J. Mach. Learn. Res.*, vol. 12, pp. 2825–2830, Dec. 2011.

**SHAMSUL AREFEEN AL MAHMUD** received the B.Sc. degree in electrical engineering from United International University, Bangladesh, in 2015, and the M.Sc. degree in autonomous systems from Aalto University, Finland, and from the KTH Royal Institute of Technology, Sweden, in 2020. Currently, he is pursuing the Ph.D. degree with the Department of Electronics and Nanoengineering, School of Electrical Engineering, Aalto University. His main research interest includes electronics and wireless power transfer systems.

**PRASAD JAYATHURATHNAGE** (Member, IEEE) received the B.Sc. degree in electronics and telecommunications engineering from the University of Moratuwa, Sri Lanka, in 2009, and the Ph.D. degree in electrical and electronic engineering from Nanyang Technological University, Singapore, in 2017. He is working at the Queensland University of Technology, Australia, and the Rolls-Royce-NTU Corporate Laboratory, Singapore. He is currently a Postdoctoral Researcher with the School of Electrical Engineering, Aalto University, Espoo, Finland. His research interests include high-frequency power converters, wide-band-gap devices, and wireless power transfer.

**SERGEI A. TRETYAKOV** (Fellow, IEEE) received the Diploma degree in engineering, the Ph.D. degree in sciences, and the D.Sc. degree in radiophysics from Saint Petersburg State Technical University, Saint Petersburg, Russia, in 1980, 1987, and 1995, respectively. From 1980 to 2000, he was with the Department of Radiophysics, Saint Petersburg State Technical University. He is currently a Professor of radio science with the Department of Electronics and Nanoengineering, Aalto University, Espoo, Finland. He has authored or coauthored six research monographs and over 300 journal articles. His current research interests include electromagnetic field theory, complex media electromagnetics, metamaterials, and microwave engineering. He was the Chairperson of the Saint Petersburg IEEE Transactions on Electron Devices, IEEE Transactions on Microwave Theory and Techniques, and the Antennas and Propagation Chapter, from 1995 to 1998, and the General Chair of the International Congress Series on Advanced Electromagnetic Materials in Microwaves and Optics (Metamaterials) and the President of the Virtual Institute for Artificial Electromagnetic Materials and Metamaterials (Metamorphose VI), from 2007 to 2013.